Unravelling Mangrove Biophysical Feedback on Rapidly Prograding Delta by Integration of UAV and Satellite Imagery

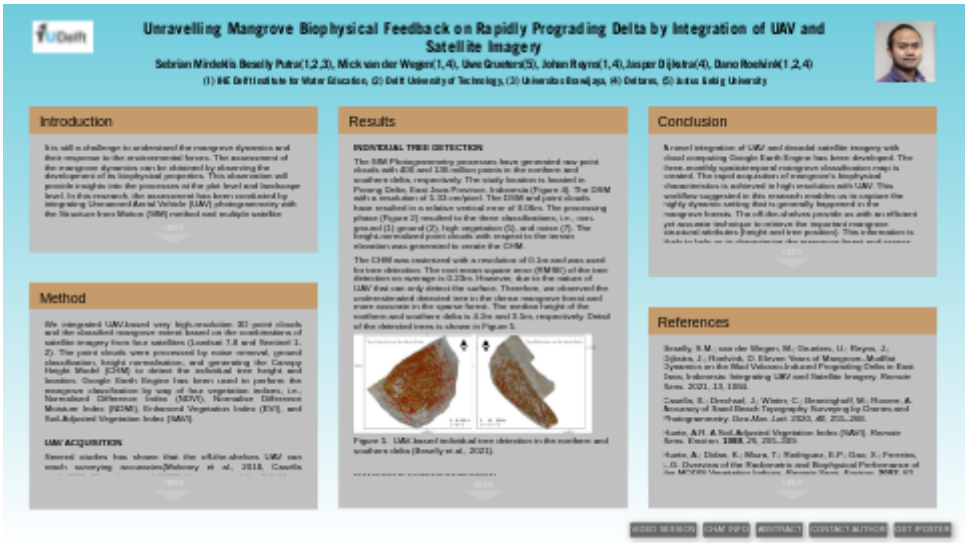

Sebrian Mirdeklis Beselly Putra(1,2,3), Mick van der Wegen(1,4), Uwe Grueters(5), Johan Reyns(1,4), Jasper Dijkstra(4), Dano Roelvink(1,2,4)

(1) IHE Delft Institute for Water Education, (2) Delft University of Technology, (3) Universitas Brawijaya, (4) Deltares, (5) Justus Liebig University

PRESENTED AT:

INTRODUCTION

It is still a challenge to understand the mangrove dynamics and their response to the environmental forces. The assessment of the mangrove dynamics can be obtained by observing the development of its biophysical properties. This observation will provide insights into the processes at the plot level and landscape level. In this research, the assessment has been conducted by integrating Unmanned Aerial Vehicle (UAV) photogrammetry with the Structure from Motion (SfM) method and multiple satellite imagery sources. The objectives are to retrieve the mangrove biophysical properties based on the UAV observation and estimate the extent and the age-height relationship of the mangrove forests for twelve years. The analysis resulted in an accurate individual tree structure and mangrove age distribution.

METHOD

We integrated UAV-based very high-resolution 3D point clouds and the classified mangrove extent based on the combinations of satellite imagery from four satellites (Landsat 7-8 and Sentinel 1-2). The point clouds were processed by noise removal, ground classification, height normalisation, and generating the Canopy Height Model (CHM) to detect the individual tree height and location. Google Earth Engine has been used to perform the mangrove classification by way of four vegetation indices, i.e., Normalised Difference Index (NDVI), Normalise Difference Moisture Index (NDMI), Enhanced Vegetation Index (EVI), and Soil-Adjusted Vegetation Index (SAVI).

UAV ACQUISITION

Several studies has shown that the off-the-shelves UAV can reach surveying accuracies(Moloney et al., 2018, Casella et.al.,2020, Mazzoleni et al.,2020). Here we used the DJI Mavic Pro with a flight altitude of 60m with front overlap 80% and 75% side overlap. It is equal to the orthomosaic resolution of 2.66cm/pixel. This technique can reach centi-to-decimetres accuracy as long it has a minimum of five Grounc Control Points (GCPs). Due to the limitation of the flight time, we divided the study area into several grids. Each grid is equal to 2ha and on average has 200 photos.

UAV DATA PROCESSING

The Structure from Motion (SfM) Photogrammetry technique was employed to generate the high-density point clouds. The point clouds from SfM still contain noise, therefore the processing procedure should be conducted to ensure the quality of the point clouds. Here we developed the workflow of three phases: Pre-Processing, Processing, and Post-Processing. Figure 1 below shows the workflow of the UAV data processing.

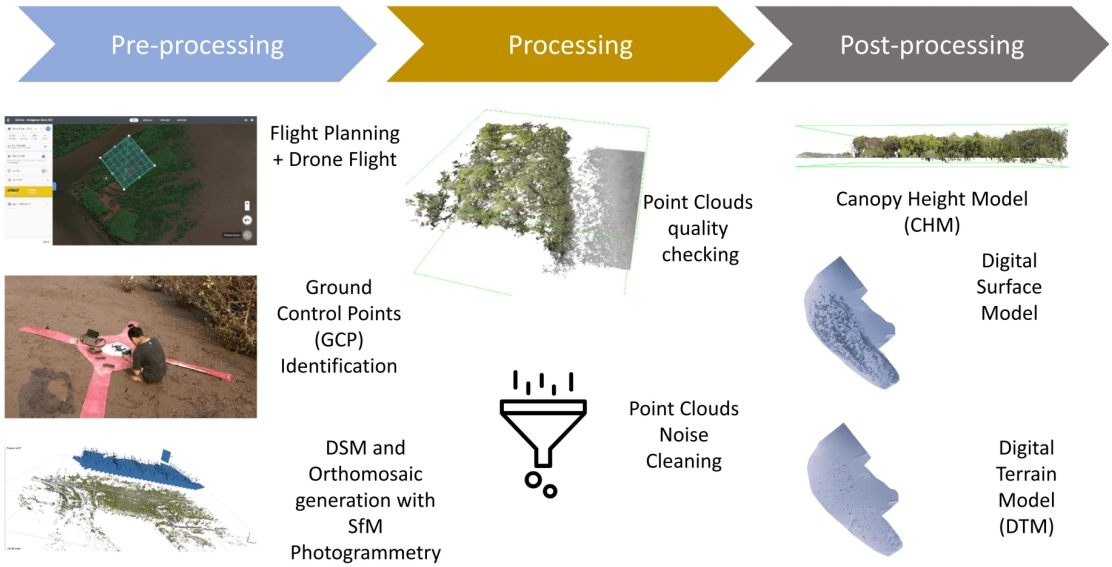

Figure 1. UAV Data Processing Workflow (adapted from Beselly et.al., 2021)

Figure 1. shows the phases of the processing. In pre-processing phase, the standardization of each data acquisition. The processing phase contain the procedure to data cleaning and Digital Surface Model (DSM), Digital Terrain Model (DTM), and Canopy Height Model (CHM) creation. The processing phase consists of nine steps, as shown in Figure 2.

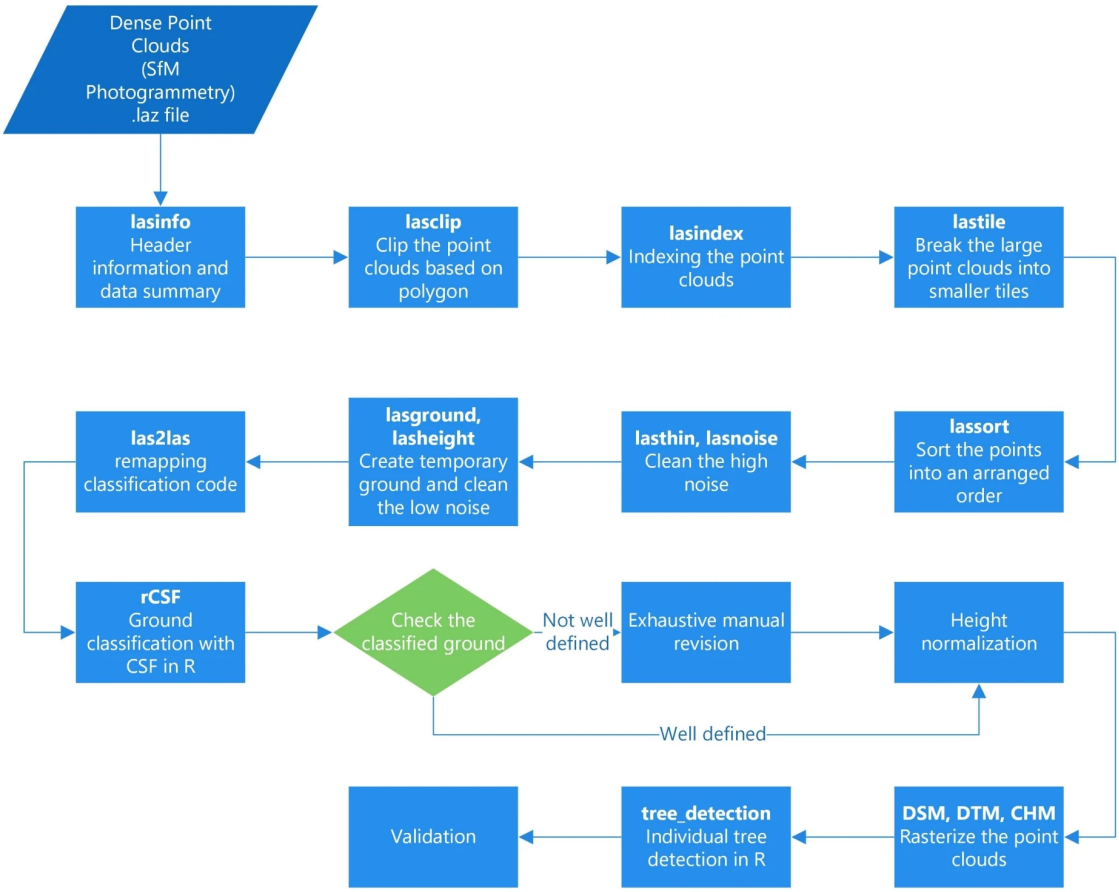

Figure 2. Processing phase workflow for the point clouds (adapted from Beselly et.al.,2021).

SATELLITE DATA PROCESSING

We used three satellite constellations for mangrove tree detection i.e., optical Satellite LANDSAT 7, LANDSAT 8, and Sentinel 2 and SAR satellite Sentinel 1. These satellite datasets were processed in Cloud Computing Google Earth Engine. We assessed the four vegetation indices, i.e., NDVI (Normalized Difference Vegetation Index) (Tucker et.al., 1979), NDMI (Normalised Difference Moisture Index) (Otero et.al., 2018), EVI (Enhanced Vegetation Index) (Huete et.al.,2002), and SAVI (Soil-Adjusted Vegetation Index) (Huete et.al.,1988). The S1 images were pre-processed with a speckle filter (Lee refined) and calculated with the mean value. The optical imageries were calculated with median value.

A supervised land cover classification was made with machine learning algorithm Random Forest (RF). The procedure of the classification is as followed: 1) training data collection, 2) classifier initiation and adjusting parameters, 3) training the classifier, 4) classifying the images, and 5) accuracy checking. Detail of the workflow is described in Figure 3.

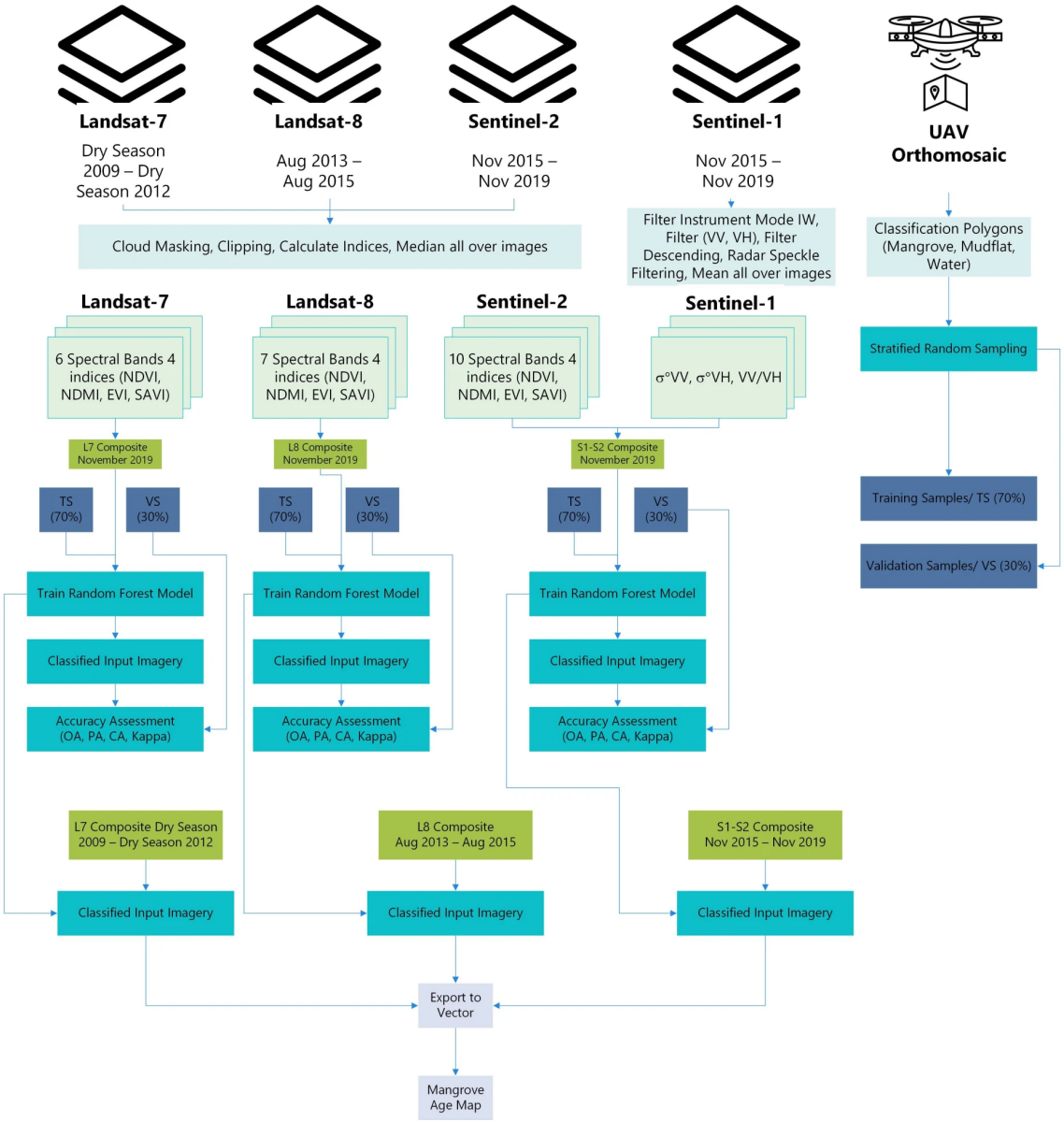

Figure 3. Satellite imagery processing workflow (adapted from Beselly et.al.,2021).

RESULTS

INDIVIDUAL TREE DETECTION

The SfM Photogrammetry processes have generated raw point clouds with 400 and 136 million points in the northern and southern delta, respectively. The study location is located in Porong Delta, East Java Province, Indonesia (Figure 4). The DSM with a resolution of 5.33 cm/pixel. The DSM and point clouds have resulted in a relative vertical error of 0.06m. The processing phase (Figure 2) resulted to the three classifications, i.e., non-ground (1) ground (2), high vegetation (5), and noise (7). The height-normalized point clouds with respect to the terrain elevation was generated to create the CHM.

The CHM was rasterized with a resolution of 0.1m and was used for tree detection. The root mean square error (RMSE) of the tree detection on average is 0.23m. However, due to the nature of UAV that can only detect the surface. Therefore, we observed the underestimated detected tree in the dense mangrove forest and more accurate in the sparse forest. The median height of the northern and southern delta is 4.2m and 3.5m, respectively. Detail of the detected trees is shown in Figure 5.

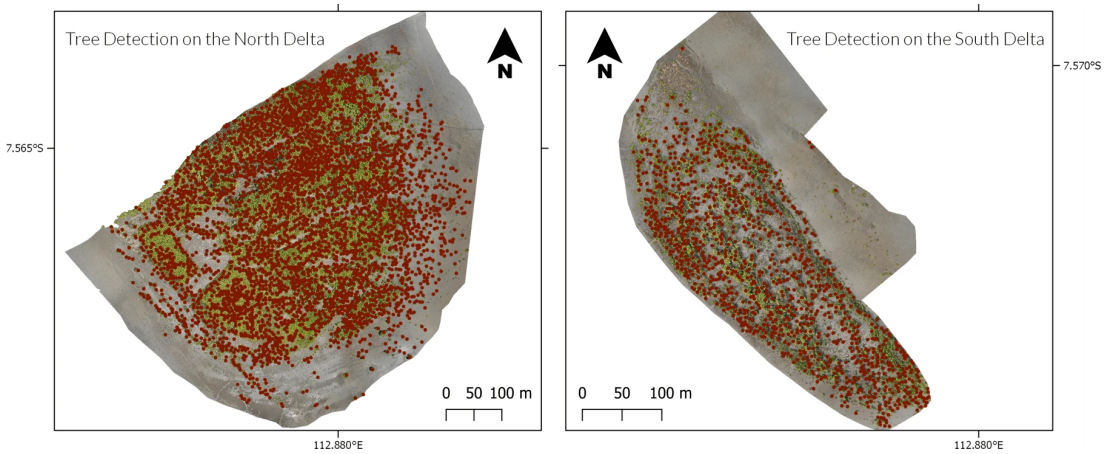

Figure 5. UAV-based individual tree detection in the northern and southern delta (Beselly et.al., 2021).

MANGROVE EXTENT DETECTION

The three-monthly mangrove classification from 2009-2019 has generated from the satellite imagery analysis in Google Earth Engine. It is clearly seen from the Figure 6. The northern delta appears earlier than the southern delta, therefore, we can observe the taller trees, which indicates the older mangrove stands.

[VIDEO] https://res.cloudinary.com/amuze-interactive/image/upload/f_auto,q_auto/v1638796387/agu-fm2021/49-e7-8b-4d-6f-75-32-e5-57-9b-c3-4b-11-01-13-0b/image/animation_npo5pi.mp4

Figure 6. Animation of the mangrove extent detection (Beselly et.al., 2021).

By taking the advantage of the three-monthly classification, we can extract the age information and analyse the development of the mangrove forest. Figure 7 shows how the development of the forest with the focus on A (larger area/ region of interest/ ROI) and B (Porong Estuary). A and B area show a positive growth trend, that varies with the season (wet and dry). However, the delta lobes' mangroves have a slightly different seasonal pattern. It is likely due to the distance to the settlement and therefore less affected by human activities.

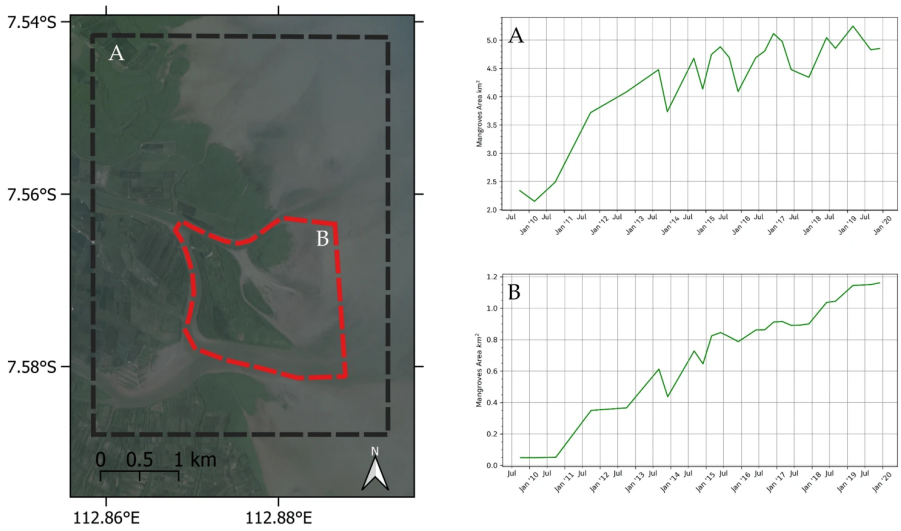

Figure 7. Time series of mangrove extent development (Beselly et.al., 2021)

Investigated further, we can see the amplitude of the high-low signal differs in the period of 2013–2017 from that in 2018–2019. In 2013–2017, we can see low mangrove extent in the wet season followed by the high regrowth in the dry season. In contrast, from 2018 to 2019, we observe only a slight decrease in the wet season and a high roughly two-fold increase in the dry season. Figure 8 reveals continuous expansion until August 2013, irrespective of the region, thus no recession is visible in both regions. From August to November 2013, there is a sudden recession, i.e., sharp decrease in the area in region A and slightly less in region B. The recession took place in the middle of the dry season and the beginning of the wet season, thus at the end of the dry season. The recovery occurred during the wet to dry season. It seems that the recession occurred at the end of the dry season while recovering and return to expansion happens in the middle of the wet season and the first half of the dry season.

It is likely in the beginning, mangroves start growing on the newly deposited, homogeneously distributed mud since its sediment attributes are rather suitable for their growth. Mangroves have access to water during the wet season as well as during the dry season. However, because of their existence, further sediment is deposited at the margin of the forest. This possibly transforms them into the basin mangrove type in certain areas, more so in the landward direction, less so on the delta lobes. When the trees start generative production, i.e., propagule production, at an age of three years seedlings that are known to be more sensitive to salt and drought might die under the extreme conditions at the end of the dry season in the basins. The delta lobes' mangroves' response to high sedimentation rates generally appears as a lack of growth instead of a decrease.

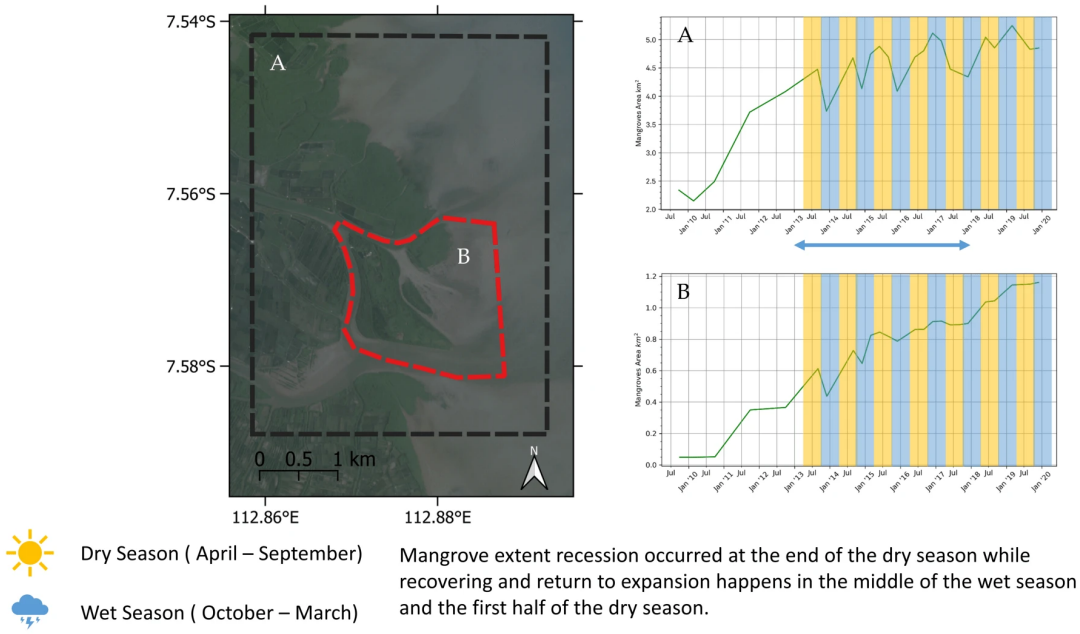

Figure 8. The mangrove forest seasonal recession and expansion (adapted from Beselly et.al.2021)

CONCLUSION

A novel integration of UAV and decadal satellite imagery with cloud computing Google Earth Engine has been developed. The three-monthly spatiotemporal mangrove classification map is created. The rapid acquisition of mangrove's biophysical characteristics is achieved in high resolution with UAV. This workflow suggested in this research enables us to capture the highly dynamic setting that is generally happened in the mangrove forests. The off-the-shelves provide us with an efficient yet accurate technique to retrieve the important mangrove structural attributes (height and tree position). This information is likely to help us to characterize the mangrove forest and assess the development or to utilize the forest for instance as coastal protection. The seasonal variation of the mangrove forests can be detected and to understand the feedback dynamics of the mangroves and the environment. Thus, the combination of the UAV and cloud-based satellite mangrove classification probably will be valuable for ecologists, coastal managers, or policymakers.

REFERENCES

Beselly, S.M.; van der Wegen, M.; Grueters, U.; Reyns, J.; Dijkstra, J.; Roelvink, D. Eleven Years of Mangrove–Mudflat Dynamics on the Mud Volcano-Induced Prograding Delta in East Java, Indonesia: Integrating UAV and Satellite Imagery. *Remote Sens.* 2021, *13*, 1084.

Casella, E.; Drechsel, J.; Winter, C.; Benninghoff, M.; Rovere, A. Accuracy of Sand Beach Topography Surveying by Drones and Photogrammetry. *Geo-Mar. Lett.* 2020, *40*, 255–268.

Huete, A.R. A Soil-Adjusted Vegetation Index (SAVI). *Remote Sens. Environ.* **1988**, *25*, 295–309.

Huete, A.; Didan, K.; Miura, T.; Rodriguez, E.P.; Gao, X.; Ferreira, L.G. Overview of the Radiometric and Biophysical Performance of the MODIS Vegetation Indices. *Remote Sens. Environ.* **2002**, *83*, 195–213.

Mazzoleni, M.; Paron, P.; Reali, A.; Juizo, D.; Manane, J.; Brandimarte, L. Testing UAV-Derived Topography for Hydraulic Modelling in a Tropical Environment. Nat. Hazards 2020, 103, 139–163.

Moloney, J.G.; Hilton, M.J.; Sirguey, P.; Simons-Smith, T. Coastal Dune Surveying Using a Low-Cost Remotely Piloted Aerial System (RPAS). *J. Coast. Res.* 2018, *345*, 1244–1255.

Otero, V.; Van De Kerchove, R.; Satyanarayana, B.; Martínez-Espinosa, C.; Fisol, M.A.B.; Ibrahim, M.R.B.; Sulong, I.; Mohd-Lokman, H.; Lucas, R.; Dahdouh-Guebas, F. Managing Mangrove Forests from the Sky: Forest Inventory Using Field Data and Unmanned Aerial Vehicle (UAV) Imagery in the Matang Mangrove Forest Reserve, Peninsular Malaysia. *For. Ecol. Manag.* **2018**, *411*, 35–45.

Tucker, C.J. Red and Photographic Infrared Linear Combinations for Monitoring Vegetation. *Remote Sens. Environ. 1979, 8*, 127–150.

ABSTRACT

It is still a challenge to understand the mangrove dynamics and their response to the environmental forces. The assessment of the mangrove dynamics can be obtained by observing the development of its biophysical properties. This observation will provide insights into the processes at the plot level and landscape level. In this research, the assessment has been conducted by integrating Unmanned Aerial Vehicle (UAV) photogrammetry with the Structure from Motion (SfM) method and multiple satellite imagery sources. The objectives are to retrieve the mangrove biophysical properties based on two periods of UAV observation (2019 and 2021) and estimate the extent and the age-height relationship of the mangrove forests for twelve years. The analysis resulted in an accurate individual tree structure and mangrove age distribution. We integrated UAV-based very high-resolution 3D point clouds and the classified mangrove extent based on the combinations of satellite imagery from four satellites (Landsat 7-8 and Sentinel 1-2). The point clouds were processed by noise removal, ground classification, height normalisation, and generating the Canopy Height Model (CHM) to detect the individual tree height and location. Google Earth Engine has been used to perform the mangrove classification by way of four vegetation indices, i.e., Normalised Difference Index, Normalised Difference Moisture Index, Enhanced Vegetation Index, and Soil-Adjusted Vegetation Index. The off-the-shelve UAV-based surface model had a total error of 0.06m compared to the ground control points, and the root mean square error of the individual tree was 0.23m. GEE's mangrove classification resulted in the three-monthly mangrove extent map —an advantage over the commonly annual mangrove extent map. The UAV-derived height information and satellite-based mangrove age class were integrated to retrieve the relationship of mangrove height dependent on the stand age. We observed the seasonal pattern of mangrove expansion. The mangroves area receded during the transition from dry to wet season and regrow during the wet to dry season. The general trend is the expansion of the mangroves with the high-low

seasonal signal that is likely related to the mangrove's response to sediment deposition and freshwater.

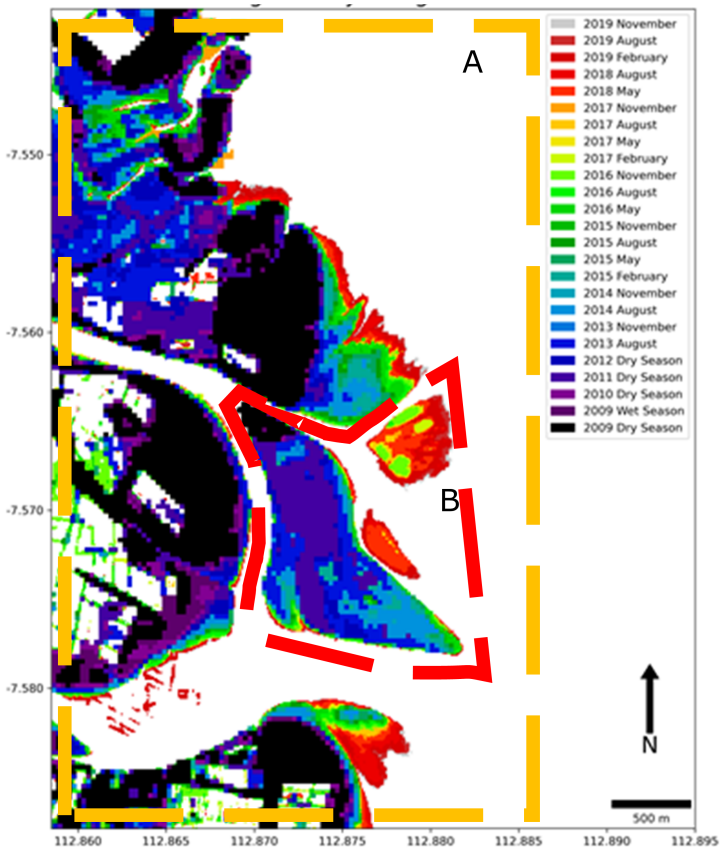

Fig 1. Three monthly mangrove extent map derived from Landsat-7,8 and Sentinel-1,2 in Google Earth Engine. The map was generated for Porong Estuary, Indonesia.

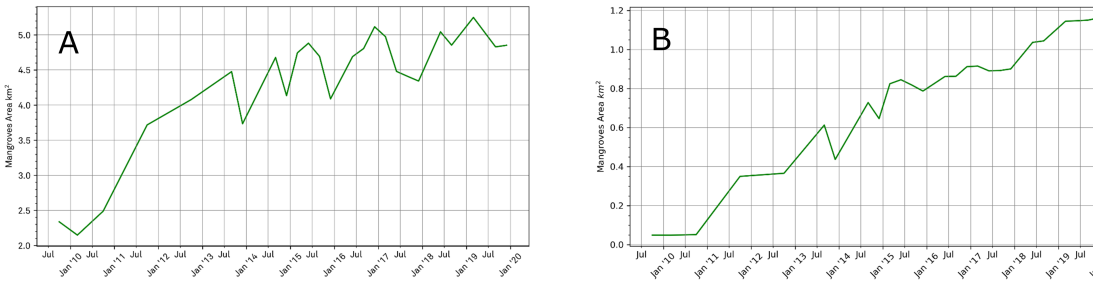

Fig 2. Mangrove extent area development in two selected areas of interest. A) larger subset to observe regional mangrove dynamics and B) the river mouth and newly developed delta mangroves

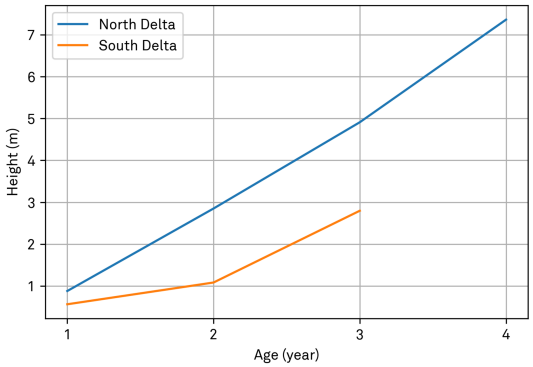

Fig 3. Age-Height map relationship based on the integration of UAV-derived CHM and satellite-derived age map. It shows different age-height relationship of the delta lobes mangroves. It indicates that the northern delta had developed earlier and so did with the mangrove succession.

(https://agu.confex.com/data/abstract/agu/fm21/8/9/Paper_934498_abstract_865769_0.png)